Quiet Connections: Reduced Fronto-Temporal Connectivity in Nondemented Parkinson's Disease During Working Memory Encoding

Alex I. Wiesman,[1,2] Elizabeth Heinrichs-Graham,[1,2] Timothy J. McDermott,[1,2] Pamela M. Santamaria,[3] Howard E. Gendelman,[1] and Tony W. Wilson[1,2,4]*

[1]*Department of Pharmacology and Experimental Neuroscience, University of Nebraska Medical Center, Omaha, Nebraska*
[2]*Center for Magnetoencephalography, University of Nebraska Medical Center, Omaha, Nebraska*
[3]*Neurology Consultants of Nebraska, Omaha, Nebraska*
[4]*Department of Neurological Sciences, University of Nebraska Medical Center, Omaha, Nebraska*

Abstract: Parkinson's disease (PD) is a common neurodegenerative disorder characterized primarily by motor symptoms such as bradykinesia, muscle rigidity, and resting tremor. It is now broadly accepted that these motor symptoms frequently co-occur with cognitive impairments, with deficits in working memory and attention being among the most common cognitive sequelae associated with PD. While these cognitive impairments are now recognized, the underlying neural dynamics and precise regions involved remain largely unknown. To this end, we examined the oscillatory dynamics and interregional functional connectivity that serve working memory processing in a group of unmedicated adults with PD and a matched group without PD. Each participant completed a high-load, Sternberg-type working memory task during magnetoencephalography (MEG), and we focused on the encoding and maintenance phases. All data were transformed into the time–frequency domain and significant oscillatory activity was imaged using a beamforming approach. Phase-coherence (connectivity) was also computed among the brain subregions exhibiting the strongest responses. Our most important findings were that unmedicated patients with PD had significantly diminished working memory performance (i.e., accuracy), and reduced functional connectivity between left inferior frontal cortices and left supramarginal–superior temporal cortices compared to participants without PD during the encoding phase of working memory processing. We conclude that patients with PD have reduced neural interactions between left prefrontal executive circuits and temporary verbal storage centers in the left supramarginal/superior temporal cortices during the stimulus encoding phase, which may underlie their diminished working memory function. *Hum Brain Mapp 37:3224–3235, 2016.* © 2016 Wiley Periodicals, Inc.

Key words: cortical oscillations; phase synchronization; magnetoencephalography; local field potentials

---

*Correspondence to: Tony W. Wilson; Center for Magnetoencephalography, 988422 Nebraska Medical Center, Omaha, NE 68198-8422, USA. E-mail: Tony.W.Wilson@gmail.com

INTRODUCTION

Parkinson's disease (PD) is a neurodegenerative disorder most commonly characterized by tremor, rigidity, akinesia or bradykinesia, and postural instability [Jankovic, 2008]. Along with motor dysfunction, PD progression often results in significant nonmotor deficiencies, including cognitive impairments [Dubois and Pillon, 1996; Jankovic, 2008; Narayanan et al., 2013; Chiaravalloti et al., 2014]. One domain of cognitive function that appears to be particularly affected is working memory, as several studies have shown that patients with PD exhibit significant deficits relative to age-matched controls during various tasks that utilize working memory [Morris et al., 1988; Owen et al., 1997; Lewis et al., 2003; Chiaravalloti et al., 2014; Trujillo et al., 2015]. However, such findings are not entirely surprising, as working memory is known to be critically dependent on dopaminergic inputs to the prefrontal cortex (PFC), and dysfunction in this circuit is a hallmark trait of PD [Narayanan et al., 2013].

As a construct, working memory is often divided into three distinct stages of processing, which include the *encoding* of critical stimuli features, *maintenance* of the temporary representation, and ultimately the *retrieval* of the representation for task performance [Baddeley, 1992]. A number of studies have identified the neural architecture which supports working memory function in healthy subjects, and increasingly, these findings have implicated alpha frequency (8–12 Hz) activity as critical [Jensen et al., 2002; Jokisch and Jensen, 2007; Jensen and Mazaheri, 2010; Händel et al., 2011; Bonnefond and Jensen, 2012; Roux and Uhlhaas, 2014]. In particular, recent studies have identified oscillatory alpha activity in regions of the left hemisphere (e.g., prefrontal cortex) that are widely known to be involved in verbal working memory processing [Cabeza and Nyberg, 2000; Rottschy et al., 2012; Heinrichs-Graham and Wilson, 2015]. More broadly, these studies and others have strongly supported oscillatory analyses of population-level neuronal activity as an essential tool in uncovering the spatiotemporal dynamics of brain networks serving working memory processing [Bonnefond and Jensen, 2012; Heinrichs-Graham and Wilson, 2015; Proskovec et al., 2016; Wilson et al., 2016], as well as potential biomarkers of the disease process in PD and other neurological disorders [Levy et al., 2002; Brown, 2006; Heinrichs-Graham et al., 2014a, 2014b; Burciu et al., 2015; Kurani et al., 2015; Wilson et al., 2015]. Specifically, several previous studies have conducted oscillatory analyses on noninvasive magnetoencephalography (MEG) measures of population-level neural activity in patients with PD [Bosboom et al., 2006; Stoffers et al., 2008; Pollok et al., 2009, 2013; Hirschmann et al., 2011; Litvak et al., 2012; Hirschmann et al., 2013; Little et al., 2013; Oswal et al., 2013; Heinrichs-Graham et al., 2014b; Burciu et al., 2015; Kurani et al., 2015], but this work has focused on motor activity and little to no insight has been provided into the oscillatory dynamics of working memory dysfunction. In fact, no studies to date have utilized MEG to examine working memory in PD.

In this study, we utilized high-density MEG to quantify population-level neural oscillatory dynamics during verbal working memory processing in a group of unmedicated patients with PD and a closely matched group of healthy controls. Importantly, this imaging method can provide the temporal resolution necessary to differentiate the stages of working memory (e.g., encoding and maintenance), as well as adequate spatial resolution for identifying the critical brain structures. To this end, we examined the local amplitude of alpha oscillatory activity during task performance, as well as the phase coherence (i.e., functional connectivity) between brain regions serving task performance. We hypothesized that patients with PD would exhibit significant deficits in alpha oscillatory activity and/or functional connectivity across a network of left-hemispheric brain regions during verbal working memory processing.

MATERIALS AND METHODS

Participants

We enrolled 16 adults with PD and 17 adults without PD. All participants except two were right-handed. The two groups were matched on age, sex, ethnicity, and other demographic factors (see Results). All participants in this study were native English speakers and fluent readers. All patients with PD had been prescribed a regularly monitored dosage of an antiparkinsonian medication for at least 2 months prior to study enrollment, and had showed a satisfactory clinical response to the particular antiparkinsonian medication regimen. Only participants with mild-to-moderate stage PD were selected to participate in the study (Hoehn and Yahr score between 1.5 and 3; [Hoehn and Yahr, 1967; Goetz et al., 2004]). Parkinsonism was measured by a certified rater using the Unified Parkinson's Disease Rating Scale (UPDRS) in the practically defined "off" state (i.e., following at least a 12-h holiday from antiparkinsonian medications). All participants performed the task early in the morning (i.e., 08:00–09:00), and participants with PD performed the task a minimum of 12 h since their last dosage of antiparkinsonian medication. Exclusionary criteria included any medical illness affecting CNS function, neurological disorder (except PD), history of head trauma, and current substance abuse. Participants with PD who reported significant cognitive impairments, or whose medical records suggested the presence of cognitive impairments, were also excluded from the study. After complete description of the study to participants, written informed consent was obtained following the guidelines of the University of Nebraska Medical Center's Institutional Review Board, which approved the study protocol.

Experimental Paradigm

Participants were seated in a nonmagnetic chair within the magnetically shielded room (MSR) and instructed to fixate on a cross-hair presented centrally. A 19 × 13 cm grid
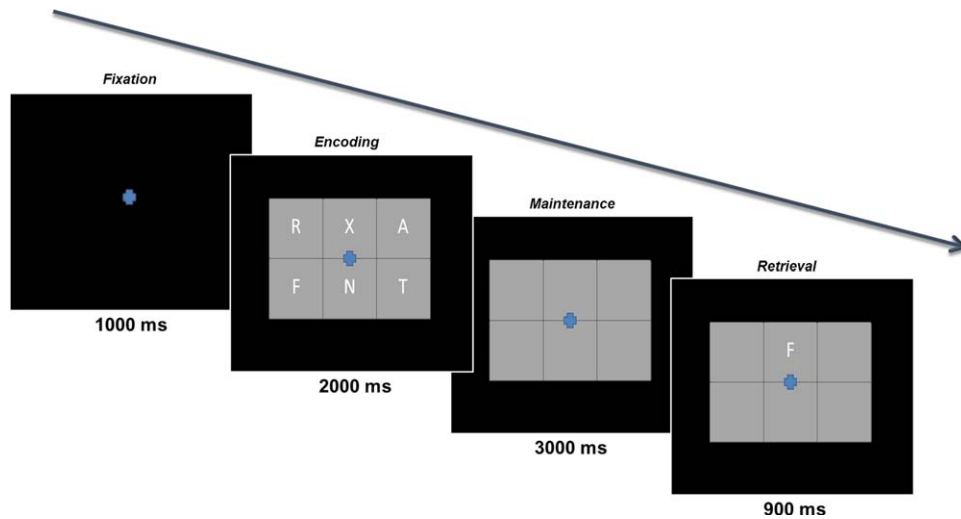
Figure 1.

Sternberg-type working memory paradigm. Each trial was composed of four periods: (1) a fixation period lasting 1.0 s, the last 0.4 s of which functioned as the baseline; (2) an encoding period lasting 2.0 s and consisting of six letters presented simultaneously within a grid; (3) a maintenance period lasting 3.0 s and consisting of the same grid without any letters; and (4) a retrieval period lasting 0.9 s and requiring participants to respond as to whether the single-letter probe being presented was included in the original encoding set. [Color figure can be viewed in the online issue, which is available at wileyonlinelibrary.com.]

(width by height) containing six letters was then presented, subtending a visual angle of approximately 10.2° horizontally and 7.0° vertically, and remained on-screen for 2 s. The letters then disappeared from the grid, and 3 s later, a single probe letter appeared. Sixty-four groups of letters were used, each with two different probe letters (a letter that was in-set and a letter that was out-of-set). These groups of letters were pseudorandomly organized such that all 64 appeared before any grouping appeared a second time, and the second presentation was always separated from the first by at least 50 letter grids. Participants were instructed to respond via button-press as to whether the probe letter was one of the six letters previously shown in the stimulus encoding grid, and no feedback was provided regarding the accuracy of their responses. Each trial lasted 6.9 s, including a 1.0 s prestimulus fixation; see Figure 1 for an illustration of the overall task design. Each participant completed 128 trials, and the task lasted approximately 14 min. Measures of accuracy (i.e., percent correct) and reaction time were recorded and used for further analysis.

MEG Data Acquisition

All recordings were conducted in a one-layer MSR with active shielding engaged. With an acquisition bandwidth of 0.1–330 Hz, neuromagnetic responses were sampled continuously at 1 kHz using an Elekta MEG system with 306 magnetic sensors, including 102 magnetometers and 204 planar gradiometers (Elekta, Helsinki, Finland). Using MaxFilter (v2.2.1; Elekta), MEG data from each subject were individually corrected for head motion and subjected to noise reduction using the signal space separation method with a temporal extension [Taulu et al., 2005; Taulu and Simola, 2006]. All analyses for this study were focused on the data collected by the 204 gradiometers. For motion correction, the position of the head throughout the recording was aligned to the individual's head position when the recording was initiated.

MEG Coregistration and Structural MRI Processing

Prior to MEG measurement, four coils were attached to the subject's head and localized, together with the three fiducial points and scalp surface, with a 3-D digitizer (Fastrak 3SF0002, Polhemus Navigator Sciences, Colchester, VT, USA). Once the subject was positioned for MEG recording, an electric current with a unique frequency label (e.g., 322 Hz) was fed to each of the coils. This induced a measurable magnetic field and allowed each coil to be localized in reference to the sensors throughout the recording session. Since coil locations were also known in head coordinates, all MEG measurements could be transformed into a common coordinate system. Each participant's MEG data were then coregistered with high-resolution structural T1-weighted MRI data prior to the application of source space analyses (i.e., beamforming) using BESA MRI (Version 2.0). These neuroanatomic images were acquired with a Philips Achieva 3 T X-series scanner using an eight-channel head coil and a 3D fast-field echo sequence with the following parameters: TR:

8.09 ms; TE: 3.7 ms; field of view: 24 cm; slice thickness: 1 mm with no gap; in-plane resolution: 1.0×1.0 mm; sense factor: 1.5. The structural volumes were aligned parallel to the anterior and posterior commissures and transformed into standardized space. Following the beamformer analyses, each subject's functional images were transformed into standardized space by using the transform that was previously applied to the structural MRI volume and spatially resampled.

MEG Time–Frequency Transformation and Statistics

Cardiac artifacts were removed from the data using signal-space projection (SSP), which was accounted for during source reconstruction [Uusitalo and Ilmoniemi, 1997]. The continuous magnetic time series was divided into epochs of 6.9 s duration, with the baseline being defined as -0.4 to 0.0 s before initial stimulus onset (Fig. 1). Epochs containing artifacts (e.g., eye blinks, muscle artifacts, eye saccades, swallowing, coughing) were rejected based on a fixed-threshold method, supplemented with visual inspection. An average of 81.82 (SD: 10.24) trials were used for further analysis. The two groups (patients and controls) did not statistically differ in the average number of trials that were used for further analysis.

Artifact-free epochs were transformed into the time–frequency domain using complex demodulation (resolution: 1.0 Hz, 50 ms; [Papp and Ktonas, 1976]), and the resulting spectral power estimations per sensor were averaged over trials to generate time–frequency plots of mean spectral density. These sensor-level data were normalized by dividing the power value of each time–frequency bin by the respective bin's baseline power, which was calculated as the mean power during the -0.4 to 0 s time period. The specific time–frequency windows used for imaging were determined by statistical analysis of the sensor-level spectrograms across the entire array of gradiometers during the 5 s "encoding" and "maintenance" time windows (Fig. 1). Each data point in the spectrogram was initially evaluated using a mass univariate approach based on the general linear model. To reduce the risk of false-positive results while maintaining reasonable sensitivity, a two-stage procedure was followed to control for Type 1 error. In the first stage, two-tailed one-sample t-tests were conducted on each data point and the output spectrogram of t-values was thresholded at $p < 0.05$ to define time–frequency bins containing potentially significant oscillatory deviations across all participants. In stage two, time–frequency bins that survived the threshold were clustered with temporally and/or spectrally neighboring bins that were also above the ($p < 0.05$) threshold, and a cluster value was derived by summing all the t-values of all data points in the cluster. Nonparametric permutation testing was then used to derive a distribution of cluster values and the significance level of the observed clusters (from stage one) were tested directly using this distribution [Ernst, 2004; Maris and Oos-

tenveld, 2007]. For each comparison, at least 10,000 permutations were computed to build a distribution of cluster values. Based on these analyses, the time–frequency windows that contained significant oscillatory events across all participants during the encoding and maintenance phases were subjected to the beamforming analysis (see Results).

MEG Source Imaging and Statistics

Cortical networks were imaged through an extension of the linearly constrained minimum variance vector beamformer [Gross et al., 2001; Hillebrand et al., 2005; Van Veen et al., 1997], which employs spatial filters in the frequency domain to calculate source power for the entire brain volume. The single images are derived from the cross-spectral densities of all combinations of MEG gradiometers averaged over the time–frequency range of interest, and the solution of the forward problem for each location on a grid specified by input voxel space. This use of the cross-spectral densities is often referred to as the dynamic imaging of coherent sources (DICS) beamformer [Gross et al., 2001]. Following convention, we computed noise-normalized, source power per voxel in each participant using active (i.e., task) and passive (i.e., baseline) periods of equal duration and bandwidth [Hillebrand et al., 2005]. Such images are typically referred to as pseudo-t maps, with units (i.e., pseudo-t) that reflect noise-normalized power differences (i.e., active vs passive) per voxel. MEG preprocessing and imaging used the Brain Electrical Source Analysis (BESA version 6.0) software.

Normalized differential source power was computed for the selected time–frequency bands (see below), using a common baseline, over the entire brain volume per participant at $4.0 \times 4.0 \times 4.0$ mm resolution. The effect of group was examined using a mixed effects analysis for the time–frequency bins of interest, in which the fixed effect was the participant groups (i.e., patients with PD and healthy controls) and the random effect was the individual subjects. As with the sensor-level analysis, a two-stage approach was used to control for Type 1 error, while maintaining reasonable sensitivity. In the first stage, two-tailed two-sample t-tests were conducted on the pseudo-t values per voxel and the output was thresholded at $p < 0.05$ to create statistical parametric maps (SPMs) showing clusters of potentially significant responses. A cluster t-value was derived in stage two, for each cluster surviving stage one, by summing all the t-values of all data points (voxels) within the cluster. Subsequently, we used permutation testing to derive a distribution of cluster t-values, and tested the observed clusters for statistical significance using this distribution [Ernst, 2004; Maris and Oostenveld, 2007]. For each comparison, at least 1,000 permutations were computed to build a distribution of cluster t-values.

Functional Connectivity Analyses

Following initial analyses, we extracted virtual sensors from the peak voxel in the three strongest left-hemispheric

clusters of the beamformer maps. The peak voxels were defined as the voxels with the maximum pseudo-t values within each cluster. These voxels were selected using the mean beamformer image across all participants and time bins, but the same clusters were observed in the averaged beamformer images of the encoding and maintenance periods (i.e., separately) across all participants. To create the virtual sensors, we applied the sensor weighting matrix derived through the forward computation to the preprocessed signal vector, which yielded a time series for the specific coordinate in source space. Note that this virtual sensor extraction was done per participant individually, once the coordinates of interest (i.e., one per cluster) were known. The virtual sensor time series from each cluster were then subjected to phase coherence analyses to examine functional connectivity across this network of brain regions.

To compute phase coherence, we extracted the phase-locking value (PLV) using the method described by Lachaux et al. [1999]. The virtual sensor signals were band-pass filtered at ±1.0 Hz, and their convolution was computed using a complex Gabor wavelet centered at the target frequency. We extracted the phase of the convolution for each time–frequency bin per trial, and then evaluated the phase relationships amongst pairs of brain regions across trials to derive the PLV for the specific pair of regions. These PLVs were then averaged across the frequency range of interest. The PLV reflects the intertrial variability of the phase relationship between pairs of brain regions as a function of time. Values close to 1 indicate strong synchronicity (i.e., phase-locking) between the two voxel time series' within the specific time–frequency bin across trials, whereas values close to 0 indicate substantial phase variation between the two signals, and thus, low synchronicity (connectivity) between the two regions. To examine connectivity differences between patients with PD and controls, the phase coherence spectrograms were baseline-corrected and examined using two-tailed two-sample t-tests for each pair of brain regions as a function of time. Briefly, we used the same two-stage statistical testing approach as was used with the sensor- and source-level analyses to control for Type 1 error. This included two-sample t-tests on each data point, followed by permutation testing on the clusters that survived the $p < 0.05$ threshold used in stage one.

RESULTS

Clinical and Behavioral Data

All participants completed the MEG working memory task; however, two participants with PD and two participants without PD were excluded due to poor task performance. In addition, one further participant with PD was discovered to have a depression diagnosis late in the study and this participant was excluded from all behavioral and MEG analyses. After exclusions, mean ages of the participants were 63.1 years for patients (range: 52–76; 3 females) and 62.2 years for controls (range: 50–75; 4 females). This difference was not significant, $t(26) = -0.29$ ($p = 0.77$). Mean disease duration among these participants with PD was 5.46 years (range: 1–9 years), and mean patient UPDRS scores were 46.38 in the "off" state (range: 17–80). Further clinical and demographic characteristics are detailed in Table I.

Consistent with previous reports [Morris et al., 1988; Owen et al., 1997; Chiaravalloti et al., 2014], participants with PD were significantly less accurate than those without PD on the working memory task ($t(26) = 3.03$, $p = 0.006$). The mean accuracy for controls was 81% (SD: 11.34%; range: 63–98%) and the mean accuracy for PD patients was 68% (SD: 11.08%; range: 56–84%). Accuracy did not significantly correlate with any of the demographic measures. Note that only correct trials were used for the MEG analyses. There were no significant differences in average reaction times (RT) between groups ($t(26) = -0.35$; $p = 0.73$); however, RT did positively correlate with age ($r(26) = 0.44$; $p = 0.019$).

Sensor-Level Analysis

Analysis of the sensor-level spectrograms in the encoding and maintenance time periods showed a significant cluster of decreased alpha (9–16 Hz) oscillatory activity that began 0.2 s after stimulus onset, and was sustained throughout the duration of the encoding period in a large cluster of parieto-occipital gradiometers (Fig. 2; $p < 0.001$, corrected). To examine these oscillations as a function of time, this significant time window was divided into four nonoverlapping 0.4 s time bins for the encoding phase (0.2–1.8 s) and one transition time bin from encoding to maintenance (1.8–2.2 s). During the maintenance period, the significant cluster of alpha activity narrowed to 9–12 Hz and was sustained throughout the maintenance phase (Fig. 2; $p < 0.001$, corrected) in parieto-occipital sensors. This time window was also split into nonoverlapping 0.4 s time bins (7 total; 2.2–5.0 s). These findings are in broad agreement with a previous report examining working memory in younger adults using MEG [Heinrichs-Graham and Wilson, 2015]. All significant time bins were subjected to a beamformer analysis to examine the spatiotemporal dynamics of working memory between the PD and control groups.

Beamformer Analysis

Sequential beamformer output images were computed for the 12 time bins described in the sensor-level analyses using the 9–16 Hz (encoding) and 9–12 Hz (maintenance) frequency ranges and a common baseline period (−0.4 to 0.0 s) of the same bandwidth. To evaluate the neural dynamics serving working memory performance, we initially examined the time course of oscillatory activity in each group. These data indicated a sharp decrease in 9–16 Hz activity that began early in the encoding phase in the bilateral occipital cortices

TABLE I. Clinical and demographic characteristics

Subject ID	Age (years)	Sex	Disease duration (years)	UPDRS off	Affected side (R/L)	PD medications (type, dose)
p01	69	M	3	52	–	CD/LD (50/200 mg)
p02	70	M	5.5	37	L	Rasagiline, Pram
p03	76	M	4	64	L	Rasagiline (1 mg), CD/LD (50/200 mg)
p04	61	M	4	23	L	Ropinirole (1 mg)
p05	60	M	1	51	R	Ropinirole (1 mg)
p06	72	F	9	17	L	Ropinirole
p07	54	F	8	48	R	Pram (2 mg), Rasagiline (1 mg)
p08	64	F	8	49	–	Ropinirole (2 mg), Rasagiline (1 mg)
p09	66	M	3	73	L	Rasagiline (1 mg), CD/LD (25/100 mg)
P10	52	M	9	80	R	CD/LD, Ropinirole
p11	52	M	6	24	R	Ropinirole (8 mg)
p12	60	M	3	49	–	CD/LD (25/100 mg), Aman (200 mg)
p13	64	M	7	36	L	CD/LD (25/100 mg), Aman

Pram = pramipexole, CD/LD = carbidopa/levodopa, Aman = amantadine.
M = male, F = female, R = right, L = left.

and cerebellum, and rapidly spread to left superior temporal regions, supramarginal, and inferior frontal gyri (Fig. 3). These decreases were largely sustained throughout the encoding phase in left fronto-temporal regions, with the frontal activity slowly dissipating during the second half of the
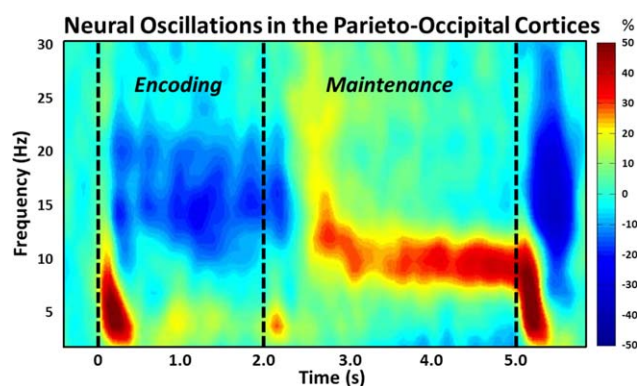

Figure 2.

Group-averaged time–frequency spectra during working memory processing. Time (in seconds) is denoted on the x-axis, with 0 s defined as the onset of the encoding grid. Frequency (Hz) is shown on the y-axis. All signal power data is expressed as a percent difference from baseline (-0.4 to 0 s), with the color legend shown to the far right. Data represent a group-averaged gradiometer sensor that was near the parietal–occipital region in each participant (the same sensor was selected in all participants). As is apparent, alpha/beta activity in this brain area strongly decreased (i.e., desynchronized) during the encoding phase, then shifted toward robust increases (i.e., synchronization) in a more narrow (alpha) band during the maintenance phase. Time periods with significant oscillatory activity (relative to baseline) were subjected to beamforming in 0.4 s nonoverlapping time bins. [Color figure can be viewed in the online issue, which is available at wileyonlinelibrary.com.]

maintenance period. Overall, the spatiotemporal dynamics of left fronto-temporal activity were generally similar in patients with PD and demographically matched older controls (Fig. 3). Likewise, both groups also exhibited alpha synchronization in the parieto-occipital cortices starting during the early maintenance phase and continuing until retrieval. Meanwhile, oscillatory responses in the right hemisphere were of much lower amplitude, largely restricted to homologue regions in the right supramarginal and prefrontal cortices, and were also comparable between the two groups. Overall, these cortical dynamics of alpha desynchronization and synchronization closely resembled those found in an earlier study of young adults [Heinrichs-Graham and Wilson, 2015].

Next, the pseudo-t maps from each participant per time–frequency bin were examined for group effects using two-tailed two-sample t-tests, with each comparison being subjected to permutation testing to control for multiple comparisons. Interestingly, after controlling for multiple comparisons at a threshold of $p = 0.05$, no significant oscillatory amplitude differences were observed between patients with PD and the control group during any time bin of the encoding or maintenance periods.

Functional Connectivity Analysis

As described in the methods, we extracted virtual sensors from the peak voxel in three clusters that showed the largest responses across all participants and time bins. These included the left dorsal prefrontal cluster (LPFC), the left supramarginal gyrus/superior temporal cluster (LSTC), and the left inferior frontal cluster (LIFC; Fig. 4). Phase-locking values were computed between these three regions for the entire time course using the 9–16 Hz frequency band. These values per node pair were then baseline corrected and subjected to two-tailed, two-sample t-tests with follow-on permutation testing to control for
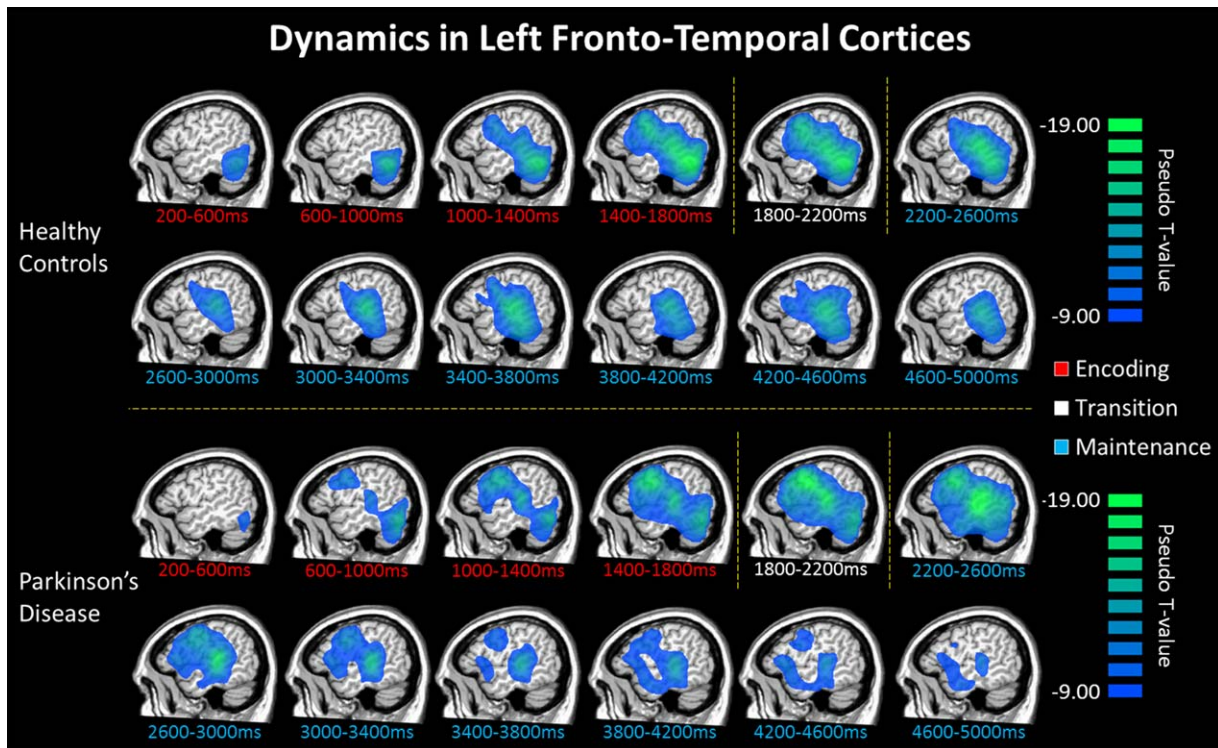
Figure 3.

Temporal dynamics of alpha oscillations in the left hemisphere. Group mean beamformer images (pseudo-*t*) of the encoding (red; 9–16 Hz), transition (white; 9–16 Hz), and maintenance (blue; 9–12 Hz) periods are shown for each 0.4 s time bin from 0.2 s after stimulus presentation until the onset of the retrieval phase. Although mean alpha amplitudes differed slightly between groups in some early (0.2–1.0 s) and late (3.4–5.0 s) time-frames, these differences did not approach significance. [Color figure can be viewed in the online issue, which is available at wileyonlinelibrary.com.]

Type 1 error, similar to the analyses previously performed on sensor- and source-level data (see Methods). No significant differences in phase-locking values were found between groups for the LIFC–LPFC or the LPFC–LSTC pathways during any time period. However, phase-locking between the LIFC and LSTC was significantly weaker in patients with PD relative to controls during much of the encoding phase, stretching from 0.3 to 1.6 s ($p = 0.008$, corrected; Fig. 5). In other words, patients with PD had reduced connectivity relative to healthy controls between the left inferior frontal cortices and left supramarginal/superior temporal cortices that began shortly (0.3 s) after the encoding grid appeared and continued until almost the end of the encoding period (Fig. 5). To ensure that these encoding differences were not due to baseline differences in the PLV between groups, we also conducted the same analyses using the absolute PLV, and our results were virtually identical ($p = 0.008$). Furthermore, we examined the absolute PLV during the baseline period for group effects and found no significant differences. Finally, for completeness, we also computed connectivity using the 9–12 Hz range, as this was the passband of interest during

the maintenance phase; the results for 9–12 Hz were also identical to those for 9–16 Hz.

DISCUSSION

Herein, we investigated the neural oscillatory dynamics that underlie working memory function in Parkinson's disease. As hypothesized, unmedicated patients with PD exhibited significantly lower accuracy on the working memory task as compared to matched controls, suggesting a deficiency in working memory-related cognitive function. Most importantly, consistent with our hypothesis of a deficit in left-hemispheric fronto-temporal circuitry, we observed a significant reduction in alpha-frequency functional connectivity between the left inferior frontal cortices and left supramarginal/superior temporal cortices in patients with PD compared to controls. This reduced connectivity began 0.3 s after stimulus presentation and persisted through most of the encoding phase of the working memory task. Of note, both these brain regions are known to be critical for verbal working memory function [Cabeza and Nyberg, 2000; Rottschy et al., 2012; Heinrichs-Graham
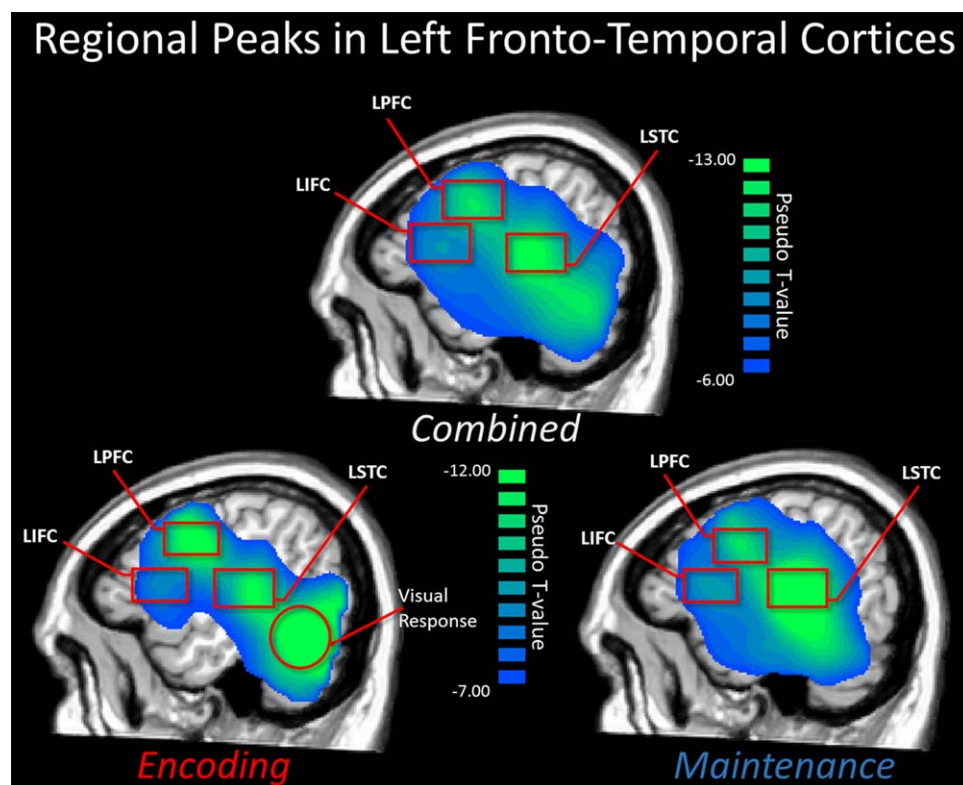
Figure 4.

Mean beamformer images used for regional peak selection. A mean beamformer image averaged across all participants and time bins (top) was utilized for identifying peak clusters and the peak voxel within each cluster, which were then subjected to connectivity analyses. The three peak regions included the left dorsal prefrontal cluster (LPFC), the left supramarginal gyrus/superior temporal cluster (LSTC), and the left inferior frontal cluster (LIFC). These left-hemispheric peaks were also observed in the mean image (across all participants) of only the encoding period (bottom left; 9–16 Hz), and in the mean image of the maintenance period (bottom right; 9–12 Hz). Note that the large posterior peak in the encoding period is the visual response elicited by the stimulus presentation, and was not included in connectivity analyses. [Color figure can be viewed in the online issue, which is available at wileyonlinelibrary.com.]

and Wilson, 2015]. In contrast to the connectivity findings, there were no differences in the amplitude of oscillatory responses between the two groups, which is very interesting and indicates the importance of our connectivity findings.

Working memory is generally understood to be made-up of several semidiscrete functional components. Briefly, a central executive component serves attention and coordinates information processing [Baddeley, 1992, 2000, 2012]. The actual memory representations are thought to be temporarily stored based on their spatial or verbal features, with the verbal features being processed by a so-called phonological loop that maintains language-related memory representations, and has been strongly linked to activity in the superior temporal/supramarginal cortices [Paulesu et al., 1993; Cabeza and Nyberg, 2000; Rottschy et al., 2012]. Likewise, spatial and nonverbal stimuli are thought to be processed by a so-called visuospatial sketchpad and involve parietal cortices. Together with the episodic buffer (another component), which acts to integrate related stimuli across space and time, working memory serves the temporary storage, manipulation, and integration of incoming stimuli of interest, prior to transfer to long-term memory or degradation. Viewed in the capacity of this working memory model, the neural oscillatory patterns that we observed support that verbal working memory function is served by a widespread left-hemispheric circuit, and that connectivity in this circuit is significantly impaired in persons with PD during the encoding phase.

Oscillatory alpha activity strongly decreased in the left prefrontal and inferior frontal cortices about 1.0 s after onset of the encoding grid in both groups, and this decrease started to dissipate during maintenance. These cortices have classically been associated with attentional processes and executive functioning [Smith and Jonides, 1999; Petersen and Posner, 2012; Stuss and Knight, 2013],
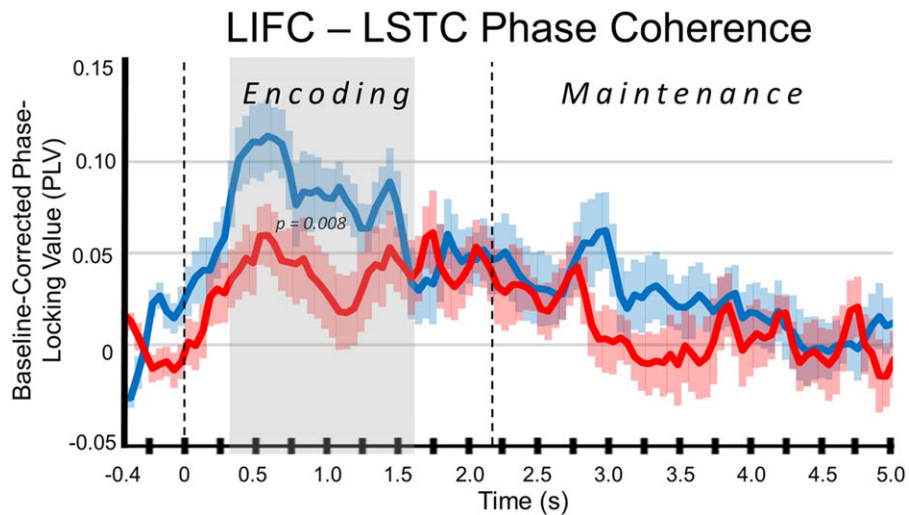
Figure 5.

Connectivity time course for the left inferior frontal and left superior temporal clusters. Mean baseline-corrected phase-locking value for connectivity between the left inferior frontal cluster (LIFC) and the left supramarginal gyrus/superior temporal cluster (LSTC) in the 9–16 Hz frequency band is shown on the y-axis. Time appears on the x-axis in seconds (s). The connectivity time course for patients with PD is shown in red, whereas that for controls appears in blue. As shown in the gray area, connectivity significantly diverged between groups during early encod-ing, and this difference lasted for the majority of the encoding phase, with controls having significantly stronger phase-coherence (connectivity) relative to patients with PD (0.3–1.6 s; $p = 0.008$). Note that the negative phase-locking values (patients only) indicate time points where connectivity between these regions was weaker than that observed during the baseline period (−0.4 to 0.0 s). [Color figure can be viewed in the online issue, which is available at wileyonlinelibrary.com.]

and neuronal activity in this area likely serves executive level processing. For example, attention to incoming stim-uli features and coordination among the relevant brain regions would be necessary to manipulate and maintain representations during the maintenance period. Many pre-vious fMRI studies have found that the left prefrontal and inferior frontal regions of the brain are particularly impor-tant for working memory tasks in humans [Smith and Jonides, 1999; Liu et al., 2009; Rottschy et al., 2012; Perl-stein et al., 2014]. During the same temporal window, a similar pattern of strong alpha decreases was observed in the left supramarginal gyrus/superior temporal region in each group. These regions have been implicated as critical to the functioning of the phonological loop component of working memory by fMRI meta analyses [Cabeza and Nyberg, 2000; Rottschy et al., 2012], which would be in agreement with our findings, as well as that of an earlier MEG working memory paper [Heinrichs-Graham and Wil-son, 2015]. Strengthening this claim, several studies have connected alpha decreases (i.e., event-related desynchroni-zation, or ERD) to fMRI BOLD activation [Brookes et al., 2005; Formaggio et al., 2008; Scheeringa et al., 2011] and our study would support the same link between alpha activity and activation in the fMRI sense. In summary, we observed alpha decreases in prefrontal and inferior frontal areas serving executive processing during encoding and

maintenance, concurrent with neuronal activity in the left supramarginal and superior temporal regions serving lan-guage processing, phonological loop, and rehearsal opera-tions. These spatiotemporal dynamics were generally comparable between patients with PD and controls, which was partially surprising given our hypotheses and the sig-nificant differences in working memory performance.

Although no significant differences in oscillatory ampli-tude were found between patients with PD and controls, a significant reduction in left-hemispheric functional connec-tivity was observed in the PD group during the encoding period, and this was clearly our most important finding. This reduction in functional connectivity occurred between the LIFC and LSTC in patients with PD, and began during early encoding and continued until near the onset of main-tenance. As discussed previously, inferior frontal regions have been linked to executive processing and attention function, while supramarginal/superior temporal cortices have been associated with the phonological loop component of working memory, and language processing more gener-ally. Thus, the current results indicate that functional com-munication between neural regions that serve executive processing and those thought to store memory representa-tions of verbal stimulus features was significantly impaired during the encoding phase of working memory processes, signifying a deficit in the ability of working memory

networks in patients with PD to effectively interact and transmit information during a pivotal stage of cognitive processing. Presumably, such interactions during the encoding phase serve to load the to-be-remembered features into temporary storage (i.e., phonological loop), and to initiate rehearsal processes that are needed to maintain the fidelity of the temporary representations. A breakdown at this stage would have significant consequences for performance, which would be consistent with our behavioral results. It is important to note that although we found impaired functional connectivity in the patients with PD during encoding, no significant differences in amplitude or connectivity were observed between groups during the maintenance of the stimulus features. This strongly implies that the maintenance phase of working memory remains relatively intact in PD, and that the behavioral deficits are likely a result of fewer stimuli features being successfully loaded into temporary storage at the encoding phase.

Aberrant patterns of functional connectivity have recently emerged as a topic of interest in understanding the pathological oscillatory dynamics of PD, and studies have found abnormal connectivity patterns during the resting-state [Berendse and Stam, 2007; Pollok et al., 2009; Hirschmann et al., 2011; Litvak et al., 2011; Hacker et al., 2012; Tessitore et al., 2012; Heinrichs-Graham et al., 2014a; Dubbelink et al., 2014; Rektorova et al., 2014] and during motor function [Jahanshahi et al., 2010; Litvak et al., 2012; Hirschmann et al., 2013; Little et al., 2013]. Furthermore, several of these studies have connected aberrant functional connectivity to disease progression in PD [Berendse and Stam, 2007; Dubbelink et al., 2014]. Interestingly, many regions that have been linked to these abnormal connectivity patterns are known to exhibit aberrant dopaminergic activity as a result of the disease, among them the prefrontal cortices [Narayanan et al., 2013]. Our findings complement these earlier studies, as the significant deficit in connectivity that we observed in patients with PD involved the left inferior frontal cortices, a prefrontal region known to be affected by dopaminergic depletion in PD. It is unclear, however, how dopamine would precisely interfere with connectivity between this region and supramarginal/superior temporal regions. Future studies should examine whether this deficit in connectivity is in-fact a result of dopaminergic dysfunction by utilizing pharmaco-MEG techniques and reinstating quasi-normal dopamine function in this region (i.e., by administering levodopa, etc.). Interestingly, dopaminergic projections from the substantia nigra to the striatum are those most substantially affected in PD, and lesions of the nigrostriatal pathway in mice have been shown to alter receptor expression in inhibitory interneurons of the prefrontal cortex [Gui et al., 2011]. Furthermore, firing-rate precision in some cortico-striatal neurons has been found to be reliant on the activity of dopaminergic receptors [Pawlak and Kerr, 2008]. Reductions in such precision could theoretically produce the deficits that we found in phase coherence (connectivity) involving the prefrontal cortices in PD.

Only recently have researchers attempted to temporally dissect the source of working memory impairments in PD, in an effort to determine the affected phase. One recent behavioral study by Chiaravalloti et al. [2014] found that, when compared to matched controls, participants with PD had a lowered ability to learn and remember a list of 10 semantically related words. However, once sufficient training was implemented (i.e., once the groups were equated for learning ability), the two groups performed equally well, signifying that the previously reported deficits lie in the acquisition and not the retrieval of these verbal stimuli. Our findings strongly support the notion that working memory impairments in PD are a result of acquisition deficits, and may be a direct repercussion of reduced functional connectivity between prefrontal and supramarginal areas during encoding. Furthermore, we found no group differences on MEG measures during the maintenance phase, and this included the widely reported parieto-occipital alpha synchronization, which is thought to be a mechanism by which memory representations are protected against incoming visual information [Jensen et al., 2002; Jokisch and Jensen, 2007; Jensen and Mazaheri, 2010; Händel et al., 2011; Bonnefond and Jensen, 2012]. We propose that such occipital activity is normal in PD, but that encoding deficits preclude all six stimuli (letters) from being successfully established as temporary representations.

Although our current findings provide critical new insight regarding the oscillatory dynamics and neural connectivity deficits during working memory processing in PD, it is important to reference the limitations of our study. First, the symptomatology of PD varies greatly across patients, so the findings of this study likely highlight the most substantial effects, and future studies of verbal working memory in PD might use a larger sample size to uncover more subtle differences. Second, our study focused on verbal working memory and thus we cannot comment on whether similar deficits exist for spatial working memory; however, recent fMRI evidence supports the idea of deficient functional connectivity during a visuospatial working memory task in patients with PD [Trujillo et al., 2015]. In addition, it would be beneficial to implement a number of variations on the task design in future studies, to observe possible differences related to memory load and response delay on the strength of oscillatory dynamics and connectivity in patients with PD. Despite these limitations, this study contributes critical new data on the neural mechanisms that underlie working memory impairments in patients with PD.

ACKNOWLEDGMENTS

REFERENCES

Baddeley A (1992): Working memory. Science 255:556–559.

Baddeley A (2000): The episodic buffer: A new component of working memory? Trends Cogn Sci 4:417–423.

Baddeley A (2012): Working memory: Theories, models, and controversies. Annu Rev Psychol 63:1–29.

Berendse HW, Stam CJ (2007): Stage-dependent patterns of disturbed neural synchrony in Parkinson's disease. Parkinsonism Relat Disord 13:S440–S445.

Bonnefond M, Jensen O (2012): Alpha oscillations serve to protect working memory maintenance against anticipated distracters. Curr Biol 22:1969–1974.

Bosboom JLW, Stoffers D, Stam CJ, Van Dijk BW, Verbunt J, Berendse HW, Wolters EC (2006): Resting state oscillatory brain dynamics in Parkinson's disease: An MEG study. Clin Neurophysiol 117:2521–2531.

Brookes MJ, Gibson AM, Hall SD, Furlong PL, Barnes GR, Hillebrand A, Singh KD, Holliday IE, Francis ST, Morris PG (2005): GLM-beamformer method demonstrates stationary field, alpha ERD and gamma ERS co-localisation with fMRI BOLD response in visual cortex. Neuroimage 26:302–308.

Brown P (2006): Bad oscillations in Parkinson's disease. In: Riederer P, Reichmann H, Youdim MBH, Gerlach M, editors. Parkinson's Disease and Related Disorders. Vienna: Springer. pp 27–30.

Burciu RG, Ofori E, Shukla P, Planetta PJ, Snyder AF, Li H, Hass CJ, Okun M, McFarland MR, Vaillancourt DE (2015): Distinct patterns of brain activity in progressive supranuclear palsy and Parkinson's disease. Mov Disord 30:1248–1258.

Cabeza R, Nyberg L (2000): Imaging cognition II: An empirical review of 275 PET and fMRI studies. J Cogn Neurosci 12:1–47.

Chiaravalloti ND, Ibarretxe -Bilbao N, DeLuca J, Rusu O, Pena J, García -Gorostiaga I Ojeda N (2014): The source of the memory impairment in Parkinson's disease: Acquisition versus retrieval. Mov Disord 29:765–771.

Dubbelink KTO, Schoonheim MM, Deijen JB, Twisk JW, Barkhof F, Berendse HW (2014): Functional connectivity and cognitive decline over 3 years in Parkinson disease. Neurology 83:2046–2053.

Dubois B, Pillon B (1996): Cognitive deficits in Parkinson's disease. J Neurol 244:2–8.

Ernst MD (2004): Permutation methods: A basis for exact inference. Stat Sci 19:676–685.

Formaggio E, Storti SF, Avesani M, Cerini R, Milanese F, Gasparini A, Alcer M, Mucelli RP, Fiaschi A, Manganotti P (2008): EEG and fMRI coregistration to investigate the cortical oscillatory activities during finger movement. Brain Topogr 21:100–111.

Goetz CG, Poewe W, Rascol O, Sampaio C, Stebbins GT, Counsell C, Giladi N, Holloway RG, Moore CG, Wenning GK, Yahr MD, Seidl L (2004): Movement Disorder Society Task Force Report on the Hoehn and Yahr Staging Scale: Status and recommendations. The Movement Disorder Society Task Force on Rating Scales for Parkinson's disease. Movement Disorders 19:1020–1028.

Gross J, Kujala J, Hämäläinen M, Timmermann L, Schnitzler A, Salmelin R (2001): Dynamic imaging of coherent sources: Studying neural interactions in the human brain. Proc Natl Acad Sci USA 98:694–699.

Gui ZH, Zhang QJ, Liu J, Zhang L, Ali U, Hou C, Fan LL, Sun YN, Wu ZH, Hui YP (2011): Unilateral lesion of the nigrostriatal pathway decreases the response of fast-spiking interneur-ons in the medial prefrontal cortex to 5-HT 1A receptor agonist and expression of the receptor in parvalbumin-positive neurons in the rat. Neurochem Int 5:618–627.

Hacker C, Perlmutter J, Criswell S, Ances B, Snyder A (2012): Resting state functional connectivity of the striatum in Parkinson's disease. Brain 135:3699–3711.

Händel BF, Haarmeier T, Jensen O (2011): Alpha oscillations correlate with the successful inhibition of unattended stimuli. J Cogn Neurosci 23:2494–2502.

Heinrichs-Graham E, Kurz MJ, Becker KM, Santamaria PM, Gendelman HE, Wilson TW (2014a): Hypersynchrony despite pathologically reduced beta oscillations in patients with Parkinson's disease: A pharmaco-magnetoencephalography study. J Neurophysiol 112:1739–1747.

Heinrichs-Graham E, Wilson TW, Santamaria PM, Heithoff SK, Torres-Russotto D, Hutter-Saunders JA, Estes KA, Meza JL, Mosley RL, Gendelman HE (2014b): Neuromagnetic evidence of abnormal movement-related beta desynchronization in Parkinson's disease. Cereb Cortex 24:2669–2678.

Heinrichs-Graham E, Wilson TW (2015): Spatiotemporal oscillatory dynamics during the encoding and maintenance phases of a visual working memory task. Cortex 69:121–130.

Hillebrand A, Singh KD, Holliday IE, Furlong PL, Barnes GR (2005): A new approach to neuroimaging with magnetoencephalography. Hum Brain Mapp 25:199–211.

Hirschmann J, Özkurt TE, Butz M, Homburger M, Elben S, Hartmann CJ, Vesper J, Wojtecki L, Schnitzler A (2011): Distinct oscillatory STN-cortical loops revealed by simultaneous MEG and local field potential recordings in patients with Parkinson's disease. Neuroimage 55:1159–1168.

Hirschmann J, Özkurt TE, Butz M, Homburger M, Elben S, Hartmann CJ, Vesper J, Wojtecki L, Schnitzler A (2013): Differential modulation of STN-cortical and cortico-muscular coherence by movement and levodopa in Parkinson's disease. Neuroimage 68:203–213.

Hoehn M, Yahr M (1967): Parkinsonism: Onset, progression and mortality. Neurology 17:427–442.

Jahanshahi M, Jones CR, Zijlmans J, Katzenschlager R, Lee L, Quinn N, Frith CD, Lees AJ (2010): Dopaminergic modulation of striato-frontal connectivity during motor timing in Parkinson's disease. Brain 133:727–745.

Jankovic J (2008): Parkinson's disease: Clinical features and diagnosis. J Neurol Neurosurg Psychiatry 79:368–376.

Jensen O, Gelfand J, Kounios J, Lisman JE (2002): Oscillations in the alpha band (9–12 Hz) increase with memory load during retention in a short-term memory task. Cereb Cortex 12:877–882.

Jensen O, Mazaheri A (2010): Shaping functional architecture by oscillatory alpha activity: Gating by inhibition. Front Hum Neurosci 4:186.

Jokisch D, Jensen O (2007): Modulation of gamma and alpha activity during a workingmemory task engaging the dorsal or ventral stream. J Neurosci 27:3244–3251.

Kurani AS, Seidler RD, Burciu RG, Comella CL, Corcos DM, Okun MS, Mackinnon CD, Vaillancourt DE (2015): Subthalamic nucleus—sensorimotor cortex functional connectivity in de novo and moderate Parkinson's disease. Neurobiol Aging 36:462–469.

Lachaux JP, Rodriguez E, Martinerie J, Varela FJ (1999): Measuring phase synchrony in brain signals. Hum Brain Mapp 8:194–208.

Levy R, Ashby P, Hutchison WD, Lang AE, Lozano AM, Dostrovsky JO (2002): Dependence of subthalamic nucleus oscillations on movement and dopamine in Parkinson's disease. Brain 125:1196–1209.

Lewis SJ, Cools R, Robbins TW, Dove A, Barker RA, Owen AM (2003): Using executive heterogeneity to explore the nature of working memory deficits in Parkinson's disease. Neuropsychologia 41:645–654.

Little S, Tan H, Anzak A, Pogosyan A, Kühn A, Brown P (2013): Bilateral functional connectivity of the basal ganglia in patients with Parkinson's disease and its modulation by dopaminergic treatment. PLoS One 8:e82762.

Litvak V, Jha A, Eusebio A, Oostenveld R, Foltynie T, Limousin P, Zrinzo L, Hariz MI, Friston K, Brown P (2011): Resting oscillatory cortico-subthalamic connectivity in patients with Parkinson's disease. Brain 134:359–374.

Litvak V, Eusebio A, Jha A, Oostenveld R, Barnes G, Foltynie T, Limousin P, Zrinzo L, Hariz MI, Friston K, Brown P (2012): Movement-related changes in local and long-range synchronization in Parkinson's disease revealed by simultaneous magnetoencephalography and intracranial recordings. J Neurosci 32: 10541–10553.

Liu L, Deng X, Peng D, Cao F, Ding G, Jin Z, Zeng Y, Li K, Zhu L, Fan N, Deng Y, Bolger DJ, Booth JR (2009): Modality-and task-specific brain regions involved in Chinese lexical processing. J Cogn Neurosci 21:1473–1487.

Maris E, Oostenveld R (2007): Nonparametric statistical testing of EEG-and MEG-data. J Neurosci Methods 164:177–190.

Morris RG, Downes JJ, Sahakian BJ, Evenden JL, Heald A, Robbins TW (1988): Planning and spatial working memory in Parkinson's disease. J Neurol Neurosurg Psychiatry 51:757–766.

Narayanan NS, Rodnitzky RL, Uc EY (2013): Prefrontal dopamine signaling and cognitive symptoms of Parkinson's disease. Rev Neurosci 24:267–278.

Oswal A, Brown P, Litvak V (2013): Synchronized neural oscillations and the pathophysiology of Parkinson's disease. Curr Opin 26:662–670.

Owen AM, Iddon JL, Hodges JR, Summers BA, Robbins TW (1997): Spatial and non-spatial working memory at different stages of Parkinson's disease. Neuropsychologia 35:519–532.

Papp N, Ktonas P (1976): Critical evaluation of complex demodulation techniques for the quantification of bioelectrical activity. Biomed Sci Instrum 13:135–145.

Paulesu E, Frith CD, Frackowiak RS (1993): The neural correlates of the verbal component of working memory. Nature 362:342–345.

Pawlak V, Kerr JN (2008): Dopamine receptor activation is required for corticostriatal spike-timing-dependent plasticity. J Neurosci 28:2435–2446.

Perlstein WM, Carter CS, Noll DC, Cohen JD (2014): Relation of prefrontal cortex dysfunction to working memory and symptoms in schizophrenia. Am J Psychiatry 158:1105–1113.

Petersen SE, Posner MI (2012): The attention system of the human brain: 20 years after. Annu Rev Neurosci 35:73.

Pollok B, Makhloufi H, Butz M, Gross J, Timmermann L, Wojtecki L, Schnitzler A (2009): Levodopa affects functional brain networks in Parkinsonian resting tremor. Mov Disord 24:91–98.

Pollok B, Kamp D, Butz M, Wojtecki L, Timmermann L, Südmeyer M, Krause V, Schnitzler A (2013): Increased SMA–M1 coherence in Parkinson's disease—Pathophysiology or compensation? Exp Neurol 247:178–181.

Proskovec AL, Heinrichs-Graham E, Wilson TW. (2016): Aging modulates the oscillatory dynamics underlying successful working memory encoding and maintenance. Hum Brain Mapp. doi: 10.1002/hbm.23178.

Rektorova I, Krajcovicova L, Marecek R, Novakova M, Mikl M (2014): Default mode network connectivity patterns associated with visual processing at different stages of Parkinson's disease. J Alzheimers Dis 42:S217–S228.

Rottschy C, Langner R, Dogan I, Reetz K, Laird AR, Schulz JB, Fox PT, Eickhoff SB (2012): Modelling neural correlates of working memory: A coordinate-based meta-analysis. Neuroimage 60:830–846.

Roux F, Uhlhaas PJ (2014): Working memory and neural oscillations: Alpha–gamma versus theta–gamma codes for distinct WM information? Trends Cogn Sci 18:16–25.

Scheeringa R, Fries P, Petersson KM, Oostenveld R, Grothe I, Norris DG, Hagoort P, Bastiaansen MC (2011): Neuronal dynamics underlying high-and low-frequency EEG oscillations contribute independently to the human BOLD signal. Neuron 69:572–583.

Smith EE, Jonides J (1999): Storage and executive processes in the frontal lobes. Science 283:1657–1661.

Stoffers D, Bosboom JLW, Deijen JB, Wolters EC, Stam CJ, Berendse HW (2008): Increased cortico-cortical functional connectivity in early-stage Parkinson's disease: An MEG study. Neuroimage 41:212–222.

Stuss DT, Knight RT (2013): Principles of Frontal Lobe Function. Oxford University Press.

Taulu S, Simola J, Kajola M (2005): Applications of the signal space separation method. IEEE Trans Signal Process 53:3359–3372.

Taulu S, Simola J (2006): Spatiotemporal signal space separation method for rejecting nearby interference in MEG measurements. Phys Med Biol 51:1759.

Tessitore A, Amboni M, Esposito F, Russo A, Picillo M, Marcuccio L, Pellecchia MT, Vitale C, Cirillo M, Tedeschi G, Barone P (2012): Resting-state brain connectivity in patients with Parkinson's disease and freezing of gait. Parkinsonism Relat Disord 8:781–787.

Trujillo JP, Gerrits NJ, Veltman DJ, Berendse HW, van der Werf YD, van den Heuvel OA (2015): Reduced neural connectivity but increased task-related activity during working memory in de novo Parkinson patients. Hum Brain Mapp 36:1554–1566.

Uusitalo MA, Ilmoniemi RJ (1997): Signal-space projection method for separating MEG or EEG into components. Med Biol Eng Comput 35:135–140.

Van Veen BD, Van Drongelen W, Yuchtman M, Suzuki A (1997): Localization of brain electrical activity via linearly constrained minimum variance spatial filtering. IEEE Trans Biomed Eng 44:867–880.

Wilson TW, Heinrichs-Graham E, Becker KM, Aloi J, Robertson KR, Sandkovsky U, White ML, O'Neill J, Knott NL, Fox HS, Swindells S. (2015): Multimodal neuroimaging evidence of alterations in cortical structure and function in HIV-infected older adults. Hum Brain Mapp 36:897–910.

Wilson TW, Heinrichs-Graham E, Proskovec AL, McDermott TJ. Neuroimaging with magnetoencephalography: A dynamic view of brain pathophysiology. Transl Res. 2016 Jan 25. pii: S1931-5244(16)00031-1. doi: 10.1016/j.trsl.2016.01.007.